TSUNAMI FLOW CHARACTERISTICS AND DESIGN LOAD EQUATIONS FOR RESIDENTIAL BUILDINGS LOCATED AT MALAYSIAN COASTLINE

MOON WEI CHEK

UNIVERSITI SAINS MALAYSIA

2019

TSUNAMI FLOW CHARACTERISTICS AND DESIGN LOAD EQUATIONS FOR RESIDENTIAL BUILDINGS LOCATED AT MALAYSIAN COASTLINE

by

MOON WEI CHEK

Thesis submitted in fulfilment of the requirements for the degree of Doctor of Philosophy

August 2019

ACKNOWLEDGEMENT

My foremost appreciation goes to Assoc. Prof. Dr. Lau Tze Liang for his supervision and valuable commentaries throughout the entire study. This study would not have been possible to achieve the completion, without his encouragement and help regarding each experimental work. My sincere appreciation goes to my co-supervisor, Dr. Puay How Tion for his continuous guidance in the development of the VSIAM3+TM model. His selfless advice and sharing in person have enlightened me a lot for my future endeavours.

Deepest appreciation to my family especially Lum Pei Teng for their patience in providing me spiritual support throughout my study. This thesis is dedicated to them. As well, I wish to express my gratitude to those who had offered their kindness and contributions along this research journey: Lee Chee Mei, Rajaviknesswaran A/L Singaravelan, Van Tze Che, Chiew Lerk Qing, Koon Foo Siong, Liew Kok Kei, Lim Yang Soh and Tan Jun Pin.

Besides, I am blessed to have the technical assistance from the administrative and technical staffs of School of Civil Engineering: Mr. Mohd Taib Yacob, Mr. Mad Fadzil Ali and Mr. Abdullah Md Nanyan. Their technical support in this project is very much indeed. I would like to extend my acknowledgement to the financial support from the Ministry of Higher Education of Malaysia through the scholarship of MyBrain15 (MyPhD) and School of Civil Engineering, Universiti Sains Malaysia.

The experimental facilities were supported by the Ministry of Science, Technology and Innovation (MOSTI), Malaysia through ScienceFund Research Grant (04-01-05-SF0562) and JICA Project for AUN/SEED-Net through Collaborative Research for Alumni (CRA) 2013.

TABLE OF CONTENTS

LIST OF TABLES

Page

LIST OF FIGURES

Page

LIST OF ABBREVIATIONS

ASCE	American Society of Civil Engineers
CCH	City and County of Honolulu
CFD	Computational fluid dynamics
CFL	Courant number
CIP-CSL	Constrained interpolation profile–conservative semi-Lagrangian
CIP-CSL3	Third-order constrained interpolation profile–conservative semi-Lagrangian
CW	Colella-Woodward
FAVOR	Fractional Area/Volume Obstacle Representation
FEMA	Federal Emergency Management Agency
FR	Flat roof
FVM	Finite volume method
GDA	GEBCO Digital Atlas
GEBCO	Gridded Bathymetric Data Sets of General Bathymetric Chart of the Ocean
GIS	Geographic information system
GR	Gabled roof
HYMAN	Hyman
ITIC	International Tsunami Information Center
JMA	Japan Meteorological Agency
KSCOE	Korean Society of Coastal and Ocean Engineers
LES	Large Eddy Simulation
LIA	Line-integrated average
MMD	Malaysian Meteorological Department
MNTEWS	Malaysian National Tsunami Early Warning System

MOSTI	Ministry of Science, Technology and Innovation
MPS	Moving particle simulation
NILIM	National Institute for Land and Infrastructure Management
PG	Pressure gauge
PVC	Polyvinyl chloride
RANS	Reynolds-averaged Navier–Stokes equations
RC	Reinforced concrete
RMR	Rumah Mesra Rakyat
SDMBTR	Structural Design Method of Buildings for Tsunami Resistance
SGS	Subgrid-scale
SIA	Surface-integrated average
SOR	Successive over-relaxation
SPH	Smoothed particle hydrodynamics
SPNB	Syarikat Perumahan Negara Berhad
TEC	Time Evolution Converting
THINC	Tangent of hyperbola for interface capturing
TM	Temporary moment
UNESCO	United Nations Educational, Scientific and Cultural Organization
UNO	Uniform Non-oscillatory
USGS	United State Geological Survey
USM	Universiti Sains Malaysia
VIA	Volume-integrated average
VOF	Volume of fluid
VSIAM3	Volume/surface integrated average multi-moment method
WALE	Wall-Adapting Local Eddy-viscosity
WB	Wall at back
WF	Wall at front

WG	Wave gauge
WM	Wall at middle
2D	Two-dimensional
3D	Three-dimensional

LIST OF SYMBOLS

Δ	Effective grid scale
Δt	Time interval
Δx	Grid size in x direction
Δy	Grid size in y direction
Δz	Grid size in z direction
a	Water depth coefficient
A	Projected area of body normal to direction of flow
b	Width of wall
C_d	Drag coefficient
Cw	WALE model constant
D	Dead load
f	VOF function
F_b	Buoyant force
F_d	Hydrodynamic force
F_h	Hydrostatic force
F_i	Debris impact force
Fr	Froude Number
F_s	Surge force
Fx	Horizontal force
Fz	Vertical force
g	Gravitational acceleration
$\mathbf{g}$	Gravitational acceleration vector
h	Water depth/wave height
H	Depth at the origin

h_b	Bore height
h_{max}	Nominal wave height/maximum water depth
h_o	Initial water column's height
h_s	Surge height
L	Length of front wave
L_o	Initial water column's length
L_{REF}	Live load effect
m	Mass of body
n	Current time step
$\mathbf{n}$	Normal vector on the surface Γ of control volume Ω
P	Pressure
P_{max}	Maximum pressure
R	Ground elevation at maximum tsunami penetration measured from initial shoreline
t	Time
T_s	Tsunami load effect
u	Flow velocity
$\mathbf{u}$	Velocity vector
u_b	Flow velocity of bore
V	Volume displaced by a submerged structure
z	Elevation from base
Z	Storey height of building model
β	Wake clearance angle
β_o	Steepness parameter
Γ	Surface of control volume Ω
ρ	Density of water
τ	Subgrid-scale turbulence stress

$\boldsymbol{\tau}$	Stress tensor
Ω	Control volume
ν	Kinematic viscosity
ν_t	Eddy viscosity

CIRI-CIRI ALIRAN DAN PERSAMAAN BEBAN REKABENTUK TSUNAMI UNTUK BANGUNAN KEDIAMAN YANG TERLETAK DI GARIS PINGGIR LAUT MALAYSIA

ABSTRAK

Kerosakan bangunan yang disebabkan oleh tsunami telah disaksikan secara terbukti oleh tinjauan pasca tsunami di seluruh dunia, termasuk Malaysia. Setakat ini, bangunan yang terletak di garis pinggir laut Malaysia tidak dibina dan direka untuk beban tsunami dan mudah terdedah kepada ancaman tsunami masa depan. Dengan itu, eksperimen hidraulik dan simulasi berangka telah dijalankan untuk menilai impak tsunami pada bangunan kediaman satu tingkat biasa di Malaysia pada skala 1:50. Keadaan gelombang nominal dengan kes melepasi dan tanpa melepasi bumbung telah diuji untuk mengkaji kesannya dalam kombinasi dengan setiap jenis model bangunan dilengkapi dengan bukaan dan tanpa bukaan. Hasil kajian eksperimen hidraulik menunjukkan bahawa model bangunan dengan bumbung gabel mempunyai kenaikan 12% dan pengurangan 52% daripada daya teraruh pada muka depan dan belakang masing-masing. Ketika gelombang tsunami mengalir melalui model bangunan, daya teraruh di muka depan dinding dalaman meningkat sehingga 50% semasa pembukaan depan meningkat daripada 15% kepada 35%, manakala pengurangan sehingga 30% telah ditunjukkan semasa dinding dalaman berpindah dari 60 mm ke 180 mm. Bagi bahagian belakang dinding dalaman, daya saling berkaitan dengan setiap parameter bukaan depan dan belakang serta konfigurasi dinding dalaman. Bagi senario yang paling teruk di mana kedudukan dinding dalaman berhampiran dengan bukaan belakang yang lebih kecil, daya pada muka belakang di dinding dalaman meningkat sehingga 100% semasa pembukaan depan meningkat daripada 15% kepada 35%. Memandangkan cabaran dalam

mensimulasikan penyebaran gelombang tsunami dan gerakan impulsif semasa impak pada dinding menegak, satu model berangka tiga dimensi yang bertaraf tinggi (VSIAM3+TM) telah dibangunkan untuk permodelan tsunami. Berdasarkan pendekatan kombinasi dari analisis eksperimen dan berangka, persamaan empirik bagi anggaran tekanan gelombang pada muka depan dan belakang bangunan telah dicadangkan. Bagi anggaran impak tsunami pada muka depan dinding dalaman, satu kaedah baru dari sudut olakan (β) telah dicadangkan dengan mempertimbangkan kesan bukaan depan dan konfigurasi dinding dalaman. Sebaliknya, faktor tidak berdimensi nisbah bagi bukaan depan ke belakang telah dicadangkan, dengan memandangkan kesan kedua-dua bukaan depan dan belakang untuk menentukan daya maksimum pada muka belakang dinding dalaman. Dengan memandangkan kekurangan kajian terhadap impak tsunami pada dinding dalaman, hasil dalam kajian ini dipercayai akan mezahirkan pandangan baru ke arah pembangunan reka bentuk bangunan yang berdaya tahan tsunami.

TSUNAMI FLOW CHARACTERISTICS AND DESIGN LOAD EQUATIONS FOR RESIDENTIAL BUILDINGS LOCATED AT MALAYSIAN COASTLINE

ABSTRACT

Tsunami-induced damage of building has been evidentially demonstrated by the post-tsunami surveys worldwide, including Malaysia. Up to present, buildings located at Malaysian coastline are not tsunami proof and are susceptible to the future tsunami threat. Motivated by the above concerns, hydraulic experiment and numerical simulation were conducted to evaluate the tsunami impact on a Malaysian typical single-storey residential building at a reduced scale of 1:50. Nominal wave conditions with wave-overtopping and non-overtopping cases were tested to study its effects in combination with each building model type with and without opening. Hydraulic experimental results demonstrated that the building model with a gabled roof had a 12% increment and 52% reduction of the force induced on the front and back faces, respectively. As the tsunami wave flowed through a building model, the induced force on an internal wall's front face increased up to 50% as the front opening size increased from 15% to 35%, whereas a decrement up to 30% was demonstrated as the internal wall moved from 60 mm to 180 mm. For the back face of an internal wall, the force interrelated with each parameter of front and back opening and the internal wall configuration. For the worst scenario where an internal wall was positioned near a smaller back opening, the back face force on the internal wall increased up to 100% as the front opening increases from 15% to 35%. For tsunami modelling, a three-dimensional higher-order numerical model (VSIAM3+TM) was developed, in view of challenges in simulating the tsunami wave propagation and its impulsive motion during impact on a vertical wall. Based

on the combinational approach from the experimental and numerical analysis, empirical equations for wave pressure estimation on the front and back faces of a building were first proposed. For the estimation of tsunami impact on an internal wall's front face, a new measure of the wake clearance angle (β) was proposed, considering the effect of the front opening and the internal wall configuration. Conversely, a dimensionless factor of front to back opening ratio was proposed, considering the effect of both front and back openings to determine the maximum force on an internal wall's back face. As there were paucity studies on the tsunami impact on an internal wall, the findings in this study were believed to provide new insight towards the development of the design of a tsunami-resilient building.

CHAPTER 1

INTRODUCTION

1.1 An overview of tsunami occurrence

Recent years, tsunami is one of the most feared natural disasters which has been making scenes around the world and Malaysia is no exemption. The term tsunami is derived from the characters: *tsu* (meaning *harbor*) and *nami* (meaning *wave*) (Koshimura, 2019). Tsunami is a series of water waves associated with the coastal geological processes that cause a sudden disturbance on the ocean. For example, earthquakes, landslides, volcanic eruptions and even impacts from the meteorological effect have the potential to trigger a tsunami (Qiu et al., 2019). Figure 1.1 illustrates the tsunami generation mechanism caused by a submarine earthquake.

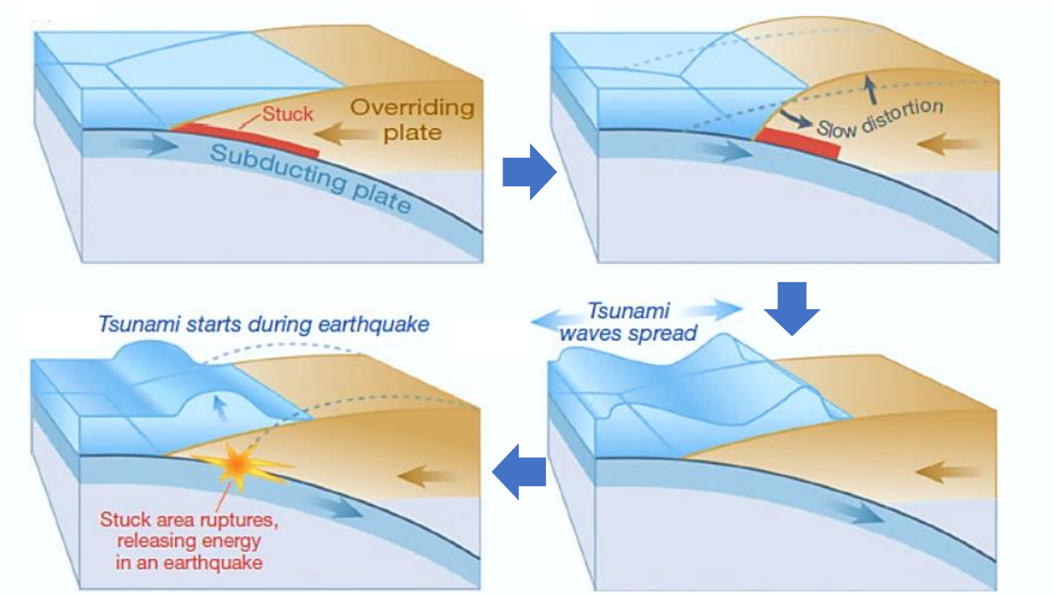

Figure 1.1 Tsunami generation mechanism caused by a submarine earthquake (Koshimura, 2019)

Based on Figure 1.1, the tsunamigenic earthquake occurs in a subduction zone, where an oceanic plate subducts beneath an overriding plate. The relative motion and the friction between the subducting and overriding plates cause the deformation of the overriding plate. As soon as the stress accumulated between the two tectonic plates reaches its limit, the overlying plate is pushed upward as a fault rupture. Finally, a tsunami wave is generated due to the vertical displacement of the seafloor. Tsunami comprises a series of long waves with wavelength up to several hundred kilometres and flow velocities of several hundred to a thousand kilometres per hour. For a typical tsunami, the water surface fluctuates near the shore with an amplitude of several meters during a short period of approximately a few minutes (Yeh et al., 2005). When tsunami wave approaches a shore, its tremendous amount of energy remains nearly constant and induces a huge force on the structures as it travels across the inundation zone.

Even though a tsunami is a rare event, its impact is devastating. There are four major tsunamis striking the coastline around the Pacific Rim: 2004 Indian Ocean tsunami, 2009 American Samoa tsunami, 2010 Chilean tsunami and 2011 Tohoku tsunami. The 2004 Indian Ocean tsunami is perhaps the most devastating tsunami in the recorded history which has claimed more than 226,226 estimated lives in several countries across the entire Indian Ocean basin (Rossetto et al., 2007). Seven years later, the 2011 Tohoku tsunami occurred on 11 March 2011, affecting almost all of the northeast coast of Japan and causing around 20,000 fatalities (Lekkas et al., 2011). Recently, the latest tsunami has occurred in September 2018, following a massive earthquake striking the Sulawesi Island. The combined effects of the tsunami and the soil liquefaction have left a destructive impact on the affected coastal communities (Omira et al., 2019).

The enormous force exerted by the tsunami could inflict great destruction to the structures, particularly buildings. The tsunami-affected buildings observed via the past tsunami events can be categorized into engineered buildings (those with proper engineering design) and non-engineered buildings that are spontaneously and informally constructed (Chock, 2013; Lekkas et al., 2011; Takahashi et al., 2011). Complete destruction has been observed for those non-engineered buildings such as the wooden buildings, whereas the engineered structures (reinforced concrete and steel buildings) behaved better. Yet, there is major and minor damage to the engineered buildings. The tsunami-induced building failure mechanisms include out-of-plan failure of a wall, tilting by scouring or collapse, overturning and large residual deformation.

Malaysian had not expected that a tsunami could strike the western shores of Peninsular Malaysia in 2004. In Malaysia, the 2004 Indian Ocean tsunami is the first and only tsunami recorded, where the major affected areas include Penang Island, Langkawi Island and Kuala Muda. A total of 68 people were killed, 6 people were missing, 300 people were injured, 1535 houses were destroyed, fishing facilities and equipment including 1332 boats were damaged during the 2004 tsunami event (Colbourne, 2005). In addition, the tsunami-caused impacts include the extensive destruction of agricultural farms and psychological trauma. In terms of the structural damage, different structural systems and construction materials have a different extent of structural damage.

Due to Malaysia lies in the "shadow" of Sumatra (as the epicenter is located to the West of Sumatra), the casualties and damage caused by the 2004 Indian Ocean tsunami are not as severe as the neighbouring countries. However, the 2004 tsunami event has changed the mindset of Malaysian citizens that the country is safe against tsunamis. As this event is one of the most critical disaster occurrences happened in the country, the tsunami prevention has gained considerable interest from the government of Malaysia to assess the tsunami threats and formulate an effective solution for reducing tsunami hazard and building a resilient society.

1.2 Problem statement

Following 2004 Indian Ocean tsunami, a number of computational simulations have been carried out by Mokhtar et al. (2008), Dao et al. (2009), Koh et al. (2009), Karim et al. (2010), Pedersen et al. (2010), Ismail and Wahab (2011), Teh et al. (2011), Shaari et al. (2013), Chai et al. (2014) and Nordin et al. (2018), focusing on the tsunami generation and propagation towards Malaysia. In Malaysia, the experimental studies on the tsunami force on the structures are only embarked in 2014 (Moon et al., 2014; Rahman et al., 2014), whereas the recent study of Mokhtar et al. (2019) experimentally investigated the tsunami bore impact on a perforated seawall. Overall, there is a paucity of the studies on the tsunami impact on a building.

The post-tsunami surveys have evidently demonstrated the building damage in the inundation zone during the 2004 Indian Ocean tsunami striking Peninsular Malaysia as shown in Figure 1.2. Kuala Muda suffers the most severe impact in terms of the building damage during 2004 tsunami event. Based on Figure 1.2, most of the damaged buildings are non-engineered (mainly masonry houses), thereby lacking the strength to withstand the tsunami force. Wall blowout and wall failure are the common damage modes that can be observed in most of the damaged buildings (Figure 1.2).

Figure 1.2 Building damage in Kuala Muda during 2004 Indian Ocean tsunami

MOSTI (2009) reported that Malaysian coastal dwellings may be under threat from a future tsunami. Yet to date, the design of a tsunami-resistant building in Malaysia still halts at the infant stage due to the lack of knowledge on tsunami impact on structures. The variability of tsunami forces is based on a site-specific basis. Without an understanding of the runup characteristics and forces of the tsunami, more lives will be claimed, and more properties will be damaged when the next tsunami hits us. Motivated by the above concern, the present study experimentally and numerically evaluates the flow characteristics of the tsunami wave striking Malaysia, with the aim of proposing the tsunami design loadings on a building.

Over the past decades, numerous researches in other tsunami-prone countries were oriented towards the tsunami forces estimation on structures, particularly buildings, focusing on simplified block models (Arabi et al., 2019; Arnason et al., 2009; Asakura et al., 2002; Bridges, 2011; Foster et al., 2017; Thomas et al., 2015; Wüthrich et al., 2019). In fact, a real building has openings and roof. Therefore, building model with different sizes of openings had also been attempted, so that the water is able to flow inside the building (Liew, 2015; Lukkunaprasit et al., 2009; Thusyanthan and Madabhushi, 2008; Wilson et al., 2009; Wüthrich et al., 2018a).

However, the afore-mentioned studies overlook the tsunami force acting on the interior part of a building, as the maximum force acts on the exterior part when a building is subjected to a tsunami wave. From the viewpoint of engineering, it is impractical to design an internal wall by using the maximum design loads for the external wall.

In fact, the tsunami force on an internal wall might be influenced by the opening (as shown in Figure 1.2), provided the external wall can resist the tsunami wave force. Up to present, the study of Triatmadja and Nurhasanah (2012) and Mizutani et al. (2014) demonstrated the effect of an internal wall on the tsunami force on a building. Although the arising researches have been carried out, there is no relationship proposed to study the effect of the spatial arrangement of an internal wall. Therefore, a generalized empirical equation is needed for the estimation of tsunami force on an internal wall, considering the effect of various openings and internal wall configurations. To successfully accomplish the research framework, this study proposes the design tsunami loads for two different categories: interior and exterior parts, so that the coastal building performs better when the next tsunami hits the coastline. The present study thus provides new insight towards the development of the design of a tsunami-resilient building instead of a tsunami-resistant building based on the consideration in term of economic aspect.

As an alternative to physical experiment, the study on tsunami force on structure has also been investigated with the aid of the numerical simulation. Throughout the years, tsunami simulation has been done by using the commercial Computational Fluid Dynamics (CFD) software (Arabi et al., 2019; Douglas and Nistor, 2015; Ghosh et al., 2016; Ghosh et al., 2019; Guler et al., 2018; Gupta et al., 2019; Hartana and Murakami, 2015; Huang and Zhu, 2015; Jiang et al., 2017; Kihara and Kaida, 2019; Qin et al., 2018; Sarjamee et al., 2017; Yang et al., 2018). Apart from the licensing cost, the limited option of choosing and changing the numerical schemes are the limitations of the commercial CFD software. Although the numerical scheme with lower-order accuracy is easy to converge, the numerical diffusion occurs (Puay, 2009; Zhang et al., 2015), results in less accuracy for the simulated results. The study of Moon et al. (2018) demonstrated that the lower-order scheme reproduces a lower propagation speed as compared to the higher-order scheme.

As tsunami flow undergoes the impulsive motion, the accuracy of the numerical model is highly dependent on the accuracy of the momentum equation solver. With continued rapid progress in the development of the numerical scheme, conservative and oscillationless higher-order schemes should be disclosed deeper for the application of tsunami wave propagation, in order to reproduce tsunami wave with accurate propagation speed and induced impact pressure. In this context, a three-dimensional numerical model with the higher-order numerical scheme is proposed to reproduce the hydraulic experiment and supplement the experimental results.

1.3 Research objectives

This study aims to experimentally and numerically study the tsunami flow characteristics and loading on the typical residential buildings in Malaysia. The specific objectives of this study are:

a. To evaluate the effect of a gabled roof and a flat roof on the tsunami flow characteristics and the induced loads on a building.

b. To experimentally investigate the characteristics of tsunami flow through a building with various openings and internal wall configurations.
c. To develop a numerical model with higher-order schemes for the wave propagation over dry-land and the wave impact on a building.
d. To propose empirical equations for estimating the tsunami loads on external and internal walls of a building.

1.4 Scope of study

In the present study, the target building prototype is a typical single-storey residential building with a gabled roof located at Malaysian tsunami-prone coastline. Prior to the execution of the hydraulic experiment, a relatively gentle slope for the tsunami-prone coastal areas in Malaysia was chosen and used for the establishment of wave flume's platform. The bed of the shore was assumed to be rigid and without friction.

In the hydraulic experiment, a dam-break mechanism was used to generate tsunami waves with 40, 70 and 100 mm nominal wave conditions, comprising the cases of wave overtopping and non-overtopping on the building model. Only tsunami runup was simulated, whereas the tsunami drawdown was not considered. Notably, the flow consisted of clean water as sediment transport was not concerned in this study. In this study, the building model was only tested with its short face towards the incoming waves, hereafter referred to as the 0° orientation. Two cases of building models with and without openings were tested separately in the hydraulic experiment.

In numerical modelling, the fluid flow was described by the Eulerian method where the fluid moves relative to the mesh. A multiphase volume of fluid (VOF)-based model was developed based on the volume/surface integrated average multi-moment method (VSIAM3) framework. In the simulation of tsunami propagation on land, supplementary scenarios with 50, 60, 80, 90 mm nominal wave conditions were simulated and only building model without opening was subjected to a tsunami wave.

1.5 Organization of thesis

This thesis is structured into five chapters. Chapter 1 begins with an overview of tsunami occurrence. The problem associated with the tsunami risk, research objectives and scope of the study was presented. Chapter 2 reviews the literature and findings related to the characteristics of tsunami bore and surge, the past major tsunami occurrence and the tsunami force on building in both experimental and numerical studies. Several numerical models are briefly introduced, together with the numerical schemes used by the previous studies. Chapter 3 summarizes the methodology and procedure, covering the experimental and numerical parts. Chapter 4 discusses the findings of the experimental study. Discussions related to the results were elucidated in terms of various nominal wave conditions, various openings, and internal wall configurations. Chapter 5 presents the numerical results and discussion, together with the proposed methodology for the tsunami force estimation on buildings. Chapter 6 underlines the conclusions of this study and proposes further recommendations for future studies.

CHAPTER 2

LITERATURE REVIEW

This chapter provides comprehensive literature pertaining to the background information of tsunami in terms of the tsunami characteristic on bore and surge and an overview of past and recent major tsunami events. The post-tsunami survey and the future tsunami occurrence in Malaysia are highlighted, followed by the tsunami design forces. The up-to-date information related to experimental and numerical studies on structure against tsunami loading is deeply elucidated in this chapter.

2.1 Tsunami characteristic on bore and surge

Tsunami, a long wave phenomenon, is characterized as a shallow water wave in the condition of water depth less than 5% of the wavelength, which is different from the wind-generated waves. However, same parameters (wave height, wave period, wavelength and phase velocity) are applied to describe both tsunami and wind generated waves. In general, tsunami could possess a wave period of 10 minutes to hours, and a wavelength of 100-500 km in an open sea, excessing 200 km in a deep ocean and mostly above 10 km (crest-to-crest distance) in coastal region (Ward and Asphaug, 2002). It is easily influenced by the diffraction and refraction as well as undergo shoaling and breaking process when approaching the coastline. In a deep sea, the initial amplitude of a tsunami is usually small (a meter or less), but it travels at high speed, with relatively small wave height. As the tsunami propagates, the amplitude of tsunami decreases for the wave energy, owing to the rate at which a wave loses its energy is inversely proportional to its wavelength (Liu et al., 2009).

As the tsunami propagates towards the shallow waters at coastal areas, it undergoes a rapid transformation, in which the speed of tsunami reduces with the increase of tsunami wave height, due to the energy loss and the total energy flux of tsunami remains constant as shown in Figure 2.1 (Nelson, 2011). According to the theory of conservation energy, the kinetic energy is converted to the potential energy as the tsunami speed slows down, and this “shoaling” effect leads to the growth of the wave height in several meters and more as the tsunami travels towards the coastal zones. On the other hand, as the tsunami approaches the shore where the water depth keeps decreasing at the runup zone, the wave rises in height and undergoes a series of wave-breaking process, or even transforms to a bore, a step-like wave with a steep breaking in front, as the tsunami breaks far offshore (Yeh and Mok, 1990).

Tsunami bore is a broken wave with infinite wavelength and uniform water depth, which is also known as surges as it rushes over the land. When the tsunami bore reaching the shoreline, the water velocity approaches the velocity of the wave propagation, leading to an accumulation of turbulence. If the energy of this high turbulence is released towards the dry shore, it could inundate the communities at coastal areas and cause severe damage (Yeh and Mok, 1990). Over the past decades, extensive efforts have been focused on the experimental investigation of the tsunami bore runup mechanism. Cross (1967) investigated the surge characteristics in terms of the shape of the measured and the theoretical surge wave. Based on the findings, the measured shape of the surge was observed to be in a good agreement with the theoretical surge profile. It was also identified that the wet-bed bore has a steeper front than that of the dry-bed surge, in accordance with the observation by Ramsden (1996).

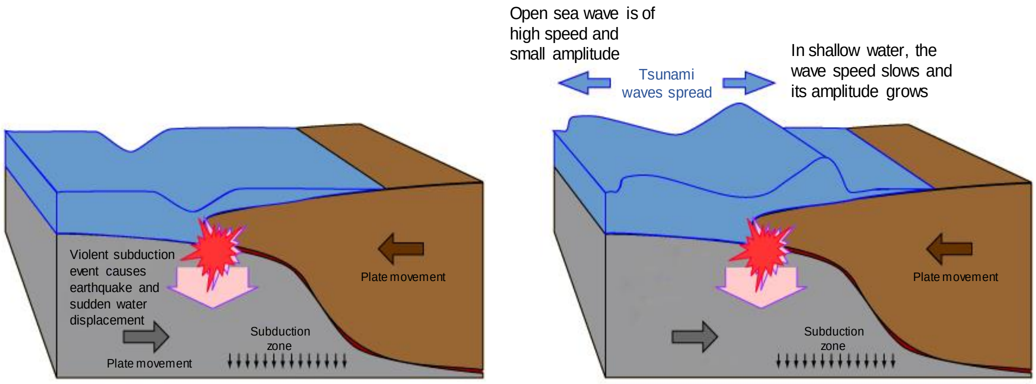

(a) (b)

Figure 2.1 Formation of tsunami wave spread

Heller et al. (2005) studied the fundamental hydraulic features of the tsunami runup through the observation of the wave surface profiles and the internal velocity distributions of the solitary wave. The wave-breaking process was classified into various stages, including the wave shoaling, front overturn and followed by the development of a bore and subsequently massive air entrainment into the wave front, as illustrated in Figure 2.2. In the study by Chanson (2006), the instantaneous free surface flow profiles of a tsunami-induced bore with floating bodies were compared to a dam-break flow on a horizontal bed. The results revealed the analogy between the propagation of tsunami-induced bores and dam-break flow.

An empirical model that predicts the bore front velocity was developed by (Murty, 1977; Kirkoz, 1983; Bryant, 2001; Matsutomi and Okamoto, 2010; FEMA P-646, 2012). The afore-mentioned studies estimated the flow velocity of the bore in terms of the bore height, as illustrated in Figure 2.3. The findings implied that the inundation flow carried numerous floating bodies with the approximately same speed as the bore, which might influence the bore characteristics. In the research of Klettner et al. (2012), wave breaking and bores formation onshore were studied. The experimental results verified that the recede of shoreline during a tsunami was due to the shoreward water drawn into the V-shaped depression wave. In addition, the hydraulic bore was observed to develop and runup on the beach when the trailing positive wave broke in the experiment. A recent investigation was conducted by Wüthrich et al. (2018b) to study the forces and moments experienced by a building subjected to both tsunami bore and surge.

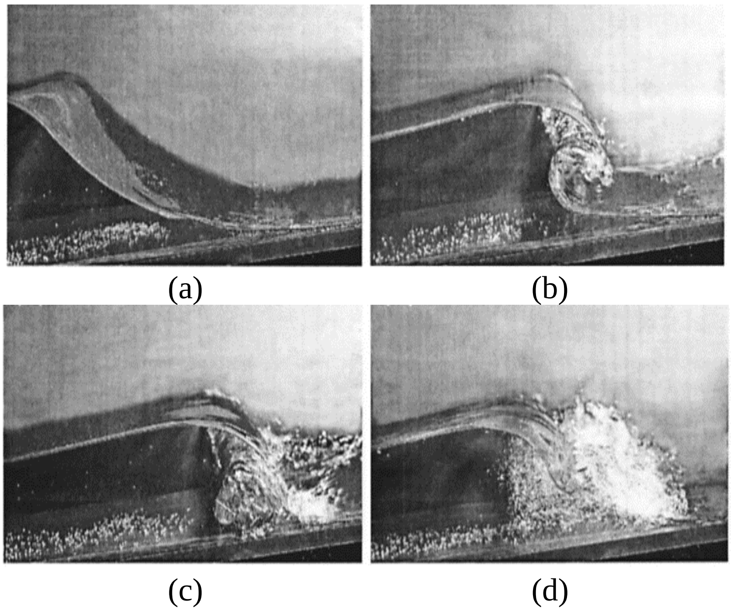

Figure 2.2 Various stage of wave breaking process: (a) Wave shoaling, (b) Front overturn, (c) Development of a bore, and (d) Massive air entrainment into wave front (Heller et al., 2005)

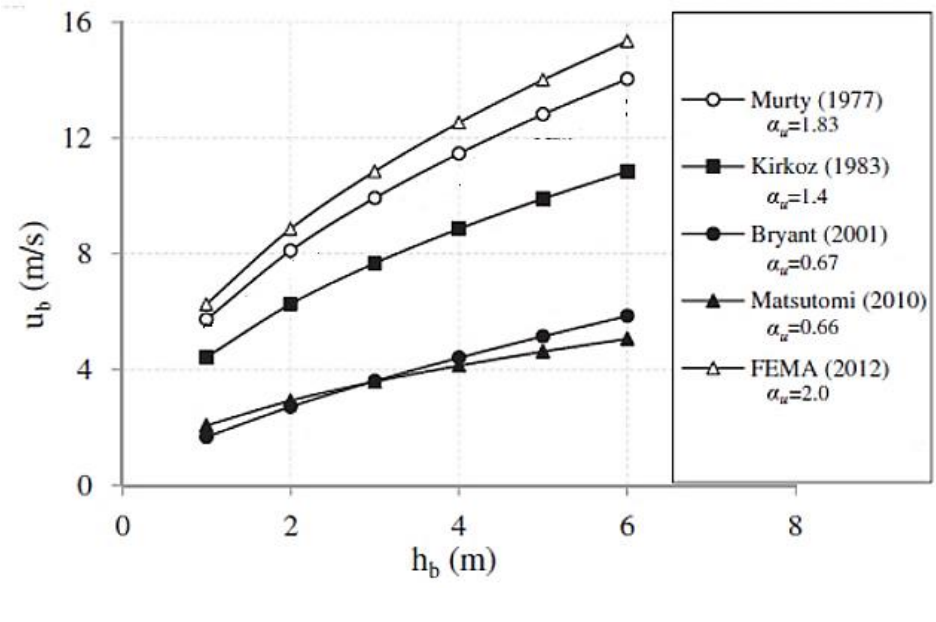

Figure 2.3 Relation between average tsunami bore velocity and bore height for different studies, prototype scale (Shafiei et al., 2016)

2.2 Past and recent major tsunami events

Since ancient time, tsunamis were observed and reported, especially in Japan, Indonesia and the Mediterranean areas. Historically from 1901 to 2016, the Pacific Ocean is the main tsunamigenic region with approximately 75% of tsunami events occurred within its basin, 10% in the Atlantic, 9% in the Mediterranean region, and followed by 6% in the Indian Ocean (Gusiakov et al., 2019). Owing to the catastrophic nature of tsunami and the huge volume of sea water released at high energy that is capable of overtopping intricately the shorelines, dams and a larger part of coastal zones, a devastating tsunami can cause a series of widespread impacts such as great damage of cars, building and infrastructures, destruction of coastal village, post-tsunami disease outbreak, and fatal consequences (Qiu et al., 2019).

Figure 2.4 depicts the historical timelines of major destructive tsunamis that causes 2000 or more deaths from 1900s to 2010s. According to Guha-Sapir et al. (2015), a total of more than 260,000 deaths (average 4600 deaths per occurrence) were reported from 58 tsunamis in 100 years. As compared with other natural disasters such as earthquakes, tornadoes, hurricanes, volcanic eruption and floods, the highest rate of fatalities was observed from tsunamis (Koshimura, 2019). Two recent tsunami events, the 2004 Indian Ocean tsunami and the 2011 Tohoku tsunami, are recognized as the most catastrophic tsunami worldwide, with the extensive destruction to the coastal area and remarkable loss of life among coastal communities.

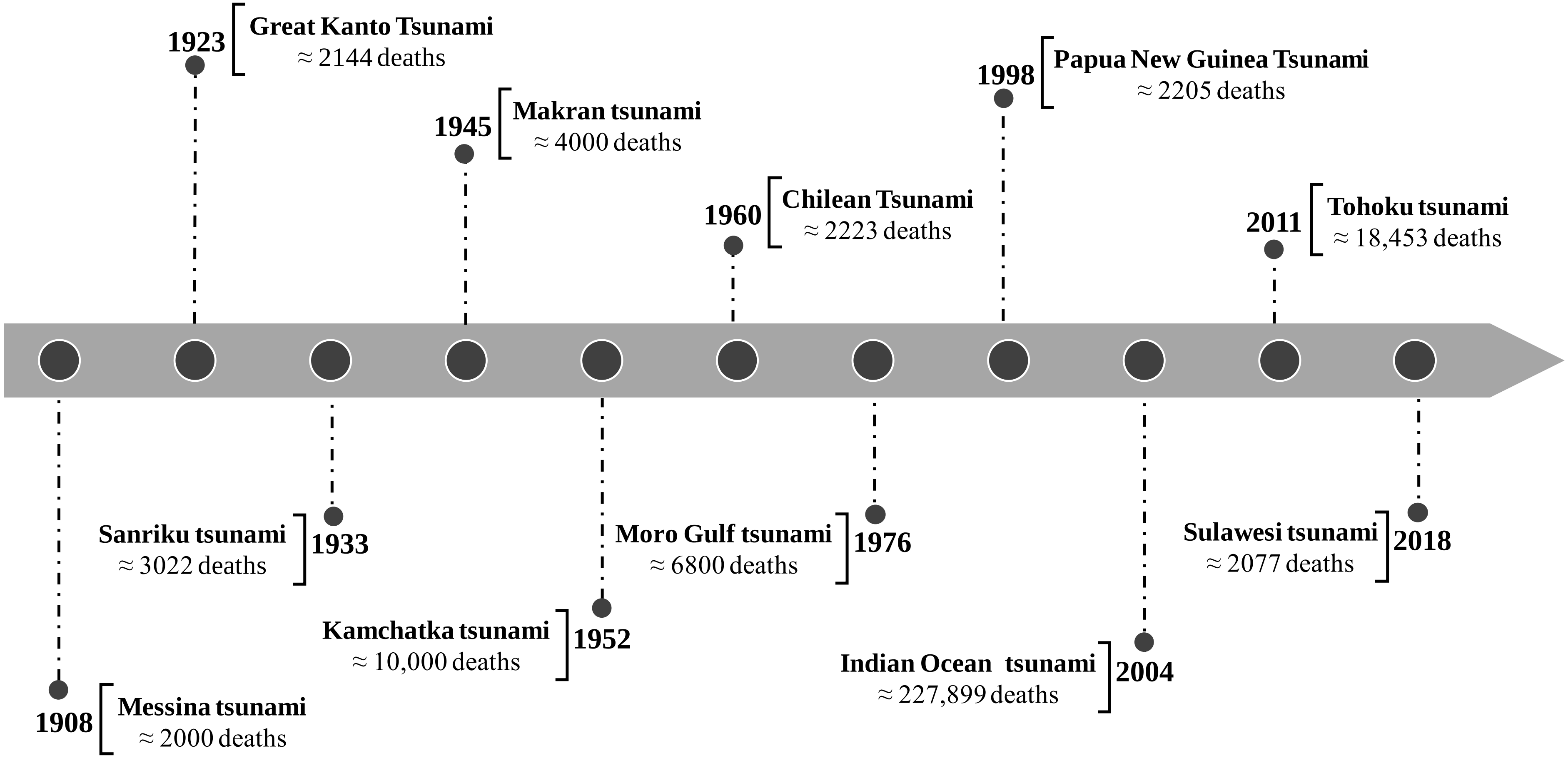

Figure 2.4 Historical timeline of major devastating tsunamis with 2000 or more fatalities from 1900s to 2010s

2.2.1 2004 Indian Ocean tsunami

Sumatra-Andaman earthquake, a devastating megathrust earthquake with a magnitude of 9.0 had occurred off the northwestern coast of Sumatra, Indonesia on 26 December 2004 (USGS, 2014). An unprecedented tsunami was generated, and the tsunami wave height was reported at 50-100 feet high along a 60 mile stretch of the northwestern coast of Sumatra, Indonesia by the International Tsunami Survey Team (Sumatra International Tsunami Survey Team, 2005). The catastrophic tsunami hit the coastal areas along the Indian Ocean within minutes, including the coast of Indonesia, Thailand, Sri Lanka and India, and Kenya in 15 minutes, 2 hours, 3 hours and 9 hours later after the earthquake, respectively (Morrow and Llewellyn, 2006).

A total of 10 nation regions including Maldives, Malaysia, Myanmar and East Africa were also affected. In order to document the effects of Indian Ocean tsunami for further building structural planning and preparedness, several survey teams had performed post-tsunami wave and runup height surveys in the south and east coast of most of the tsunami-affected regions. Table 2.1 tabulates the measured tsunami runup height at each region, presented by the survey team of Korean Society of Coastal and Ocean Engineers (KSCOE). Due to the interaction between wave and coastal topography as well as different distance from the tsunami source, the runup heights at different coastal regions were varied widely. Accordingly, the highest runup height was observed at 48.86 m in the Indian Ocean at Lampuuk Beach, Lhok Nga on the northern Sumatra.

Up to date, the 2004 Indian Ocean tsunami is categorized as the top devastating tsunami with the highest casualties (Gusiakov et al., 2019). Apparently, irreversible tsunami impacts on the structural damage of building were observed.

Owing to the difference in the type of the materials and the coastal defence structure, these buildings in the tsunami-affected areas suffered damage at different degrees, as shown in Figure 2.5. In Indonesia and Thailand, typical low-cost and residential wooden frames house along the coastal areas, constructed with corrugated steel sheet roof or tile were unconditionally disintegrated by the massive tsunami. In other words, the wooden construction materials were completely destroyed and broken down into countless pieces of wooden debris (Figure 2.5(a)).

Table 2.1 Measured tsunami runup height at each region during 2004 Indian Ocean tsunami (Choi et al., 2006)

Region	Maximum tsunami runup height (m)
Andaman-Nicobar Islands	16.50
India	11.46
Indonesia	48.86
Malaysia	7.40
Maldives	4.43
Myanmar	6.70
Sri Lanka	10.87
Thailand	19.96

According to the study of Ghobarah et al. (2006), it was reported that the 200 mm square columns in the non-engineered concrete frame structures with masonry infill had suffered significant damage, and the 50 mm thick masonry walls suffered an out-of-plane punching shear failure due to the higher tsunami forces. Due to this, tsunami waves had easily swept away all the contents of the buildings, and left the empty shells with beam, column and wall failures, resulting in a collapse of the buildings (Figure 2.5(b)). On the contrary, minor damage was found on the building with engineered and well-constructed reinforced (RC) concrete frame structures in Banda Aceh and Thailand (Figure 2.5(c)). The buildings survived from the tsunami attack and high tsunami runup levels. Besides this, a meteorological building featured with small square columns (150 mm), columns spaced (4 m), floor height (2.5-3 m), thick unreinforced infill masonry panels (100 mm), and a small number of dowel bars connecting the panels with the boundary of RC frames failed to withstand the tsunami waves height of 2.5 m or higher, and completely destroyed in Takua Pa, Phang-Nga (Figure 2.5(d)) (Lukkunaprasit and Ruangrassamee, 2008).

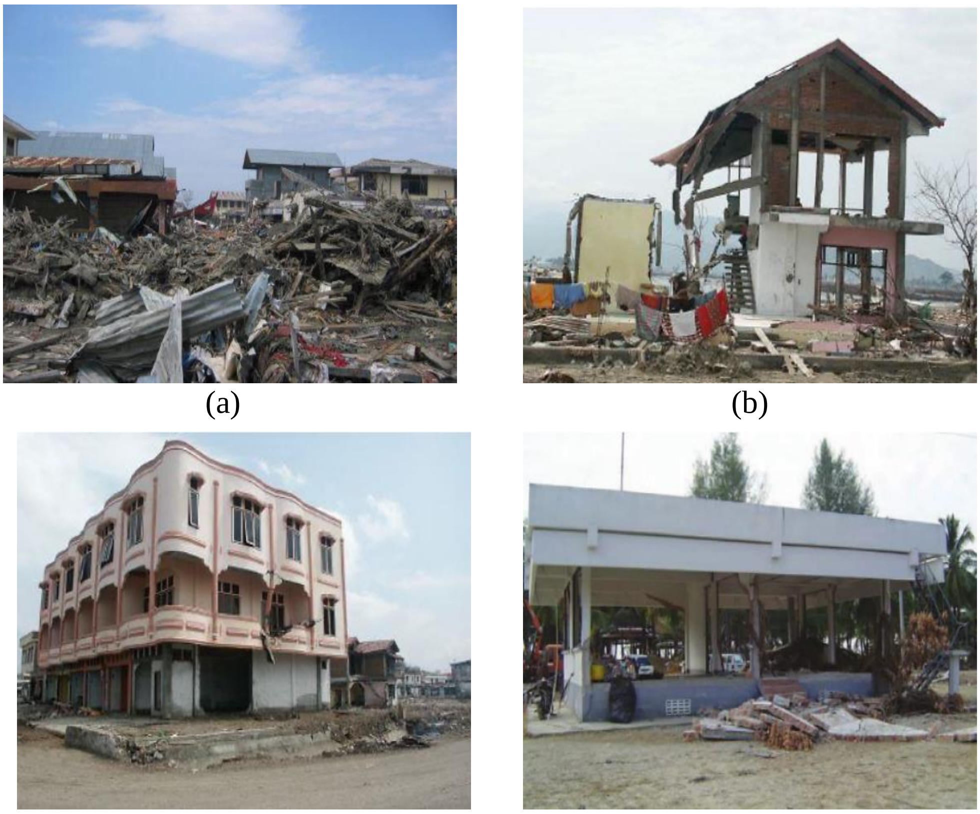

(a) (b)

(c) (d)

Figure 2.5 Tsunami impacts on the (a) wooden frame houses, (b) non-engineered lightly RC building, (c) well-constructed RC building (Gusiakov et al., 2019), and (d) RC building with unreinforced infill masonry panels (Lukkunaprasit and Ruangrassamee, 2008)

However, the majority of RC structures (2-3 storeys) survived with minor to moderate damage from collapse, in the wave heights of 3-6 m from the ground surface (Figure 2.6). As a result of the current practice of weakly connecting infill masonry panels to the boundary RC frames with widely spaced small diameter dowels (6 mm diameter at about 400 mm spacing), which serves to work well in detaching the brick walls from the frames under an excessive water pressure, thereby reducing the force transmitted to the building. This can be evidenced by the sound RC buildings in Khao Lak, the buildings withstood waves height of about 6 m from the ground, as shown in Figure 2.6(a). Likewise, a large resort building near the shoreline along the Phi Phi Don Island, had suffered non-structural damage, and the structural frames remained intact (Figure 2.6(b)).

(a) (b)

Figure 2.6 Tsunami impacts on the sound RC buildings (a) in Khao Lak, and (b) in Phi Phi Don (Lukkunaprasit and Ruangrassamee, 2008)

2.2.2 2011 Tohoku tsunami

On 11 March 2011, the Great East Japan Earthquake, the largest instrumentally recorded earthquake with a magnitude of 9.0 in Japan, occurred off the Pacific coast of Japan. Within 3 minutes of the earthquake, a tsunami warning was issued by Japan Meteorological Agency (JMA) (Hoshiba et al., 2011). The tsunami waves began striking the shores of Sanriku, continue devastating along the northeastern coastal areas of Honshu and north of Sendai, in turn trigger the largest inundation and run-up heights (Mori et al., 2011). The 2011 Tohoku tsunami have devastated all the Pacific coast in Japan impacting along the coastal cities from Hokkaido to Chiba Prefecture. In this case, approximately 18,000 casualties reported, which about 90% were associated with drowning (Satake et al., 2013). Hence, this tsunami was considered as the largest and most catastrophic tsunami event in Japan as compared to past tsunami events, 1896 Meiji tsunami and 1933 Showa Sanriku tsunami. The tsunami destruction in Japan as well as the coastlines of other countries around the Pacific Ocean such as USA and Indonesia, were rapidly broadcast worldwide. The measurement of tsunami runup height at different tsunami affected locations were reported by different survey teams, as summarized in Table 2.2.

On the Sendai Plain, the maximum tsunami wave height was recorded as 46 feet. The tsunami wave impacted the turbine building of the Fukushima Daiichi Nuclear Power Plant and striking the adjacent reactor building (Mori et al., 2011). Consequently, the radioactive core of plant's reactors suffered damage extensively, and a state of emergency which required a massive evacuation of residents living within 20 km was declared. Generally, coasts in Japan were well-protected with land tsunami countermeasures, including flood gates or sea walls to mitigate tsunami disaster. However, a post-tsunami investigation conducted by Suppasri et al. (2013) on different building and the coastal defence structures in Japan, revealed these structures were insufficient to prevent extensive overtopping by the tsunami.

It is apparent that Miyagi Prefecture was hardest hit by the tsunami, impacting the coastal dike at Watari and the disaster prevention center at Minamisanriku were destroyed badly, as shown in Figure 2.7(a) and Figure 2.7(b). There were only hospitals such as hospital at Onagawa (Figure 2.7(c)), and schools located at higher grounds found unaffected from the tsunami. Inevitably, a protective leeve with 19-foot high located at the Fukushima Daiichi Nuclear Power Plant, was also overtopped by the tsunami with the run-up heights up to 25.5 m, as shown in Figure 2.7(d) (Pararas-Carayannis, 2014). From the study of Takahashi et al. (2011), it was concluded that the complete destruction of wooden frame houses is the most typical damage during the occurrence of a tsunami.

Table 2.2 Measured tsunami runup height at each region during 2011 Tohoku tsunami (Kaistrenko et al., 2013; Lynett et al., 2013; Mori et al., 2011; Reymond et al., 2013)

Region	**Maximum tsunami runup height (m)**
Kuril Islands	5.0
French Polynesia	4.0
Galapagos Islands	6.0
Koborinai	37.9
Ryori Bay-Shirahama	23.6
Miyako	11.5
Maui and Hawaii	2.0-3.0

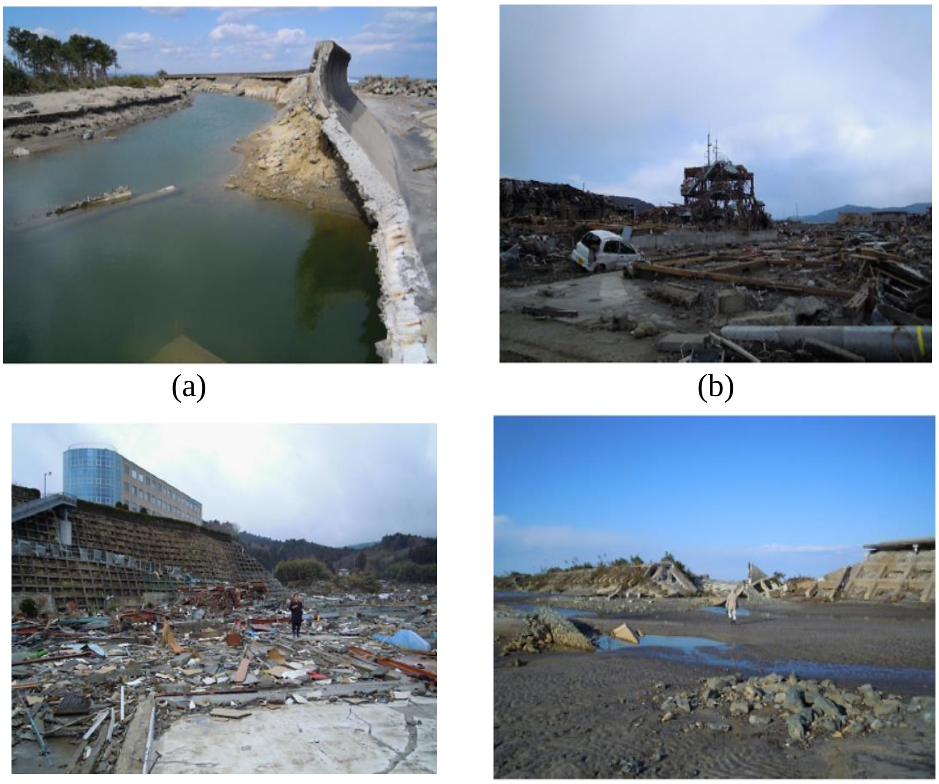

(a) (b) (c) (d)

Figure 2.7 Tsunami impacts on the (a) coastal dikes in Watari, (b) disaster prevention center at Minamisanriku and (c) hospital at Onagawa, Miyagi Prefecture, and (d) coastal dikes in Soma City, Fukushima Prefecture (Esteban et al., 2013)

In the 2011 Tohoku tsunami, the report implied that wooden frame houses were destroyed by even 2 m tsunamis (Figure 2.8(a)). As stated by Lekkas et al. (2011), the residential wooden frame houses were successfully coped with earthquake loading by absorbing the seismic energy mainly through ductile deformation. Nevertheless, they were totally hit by the wave forces from the tsunami attack. For instance, wooden houses were swept off their footings and they were carried to a great distance by the tsunami, as illustrated in Figure 2.8(b).

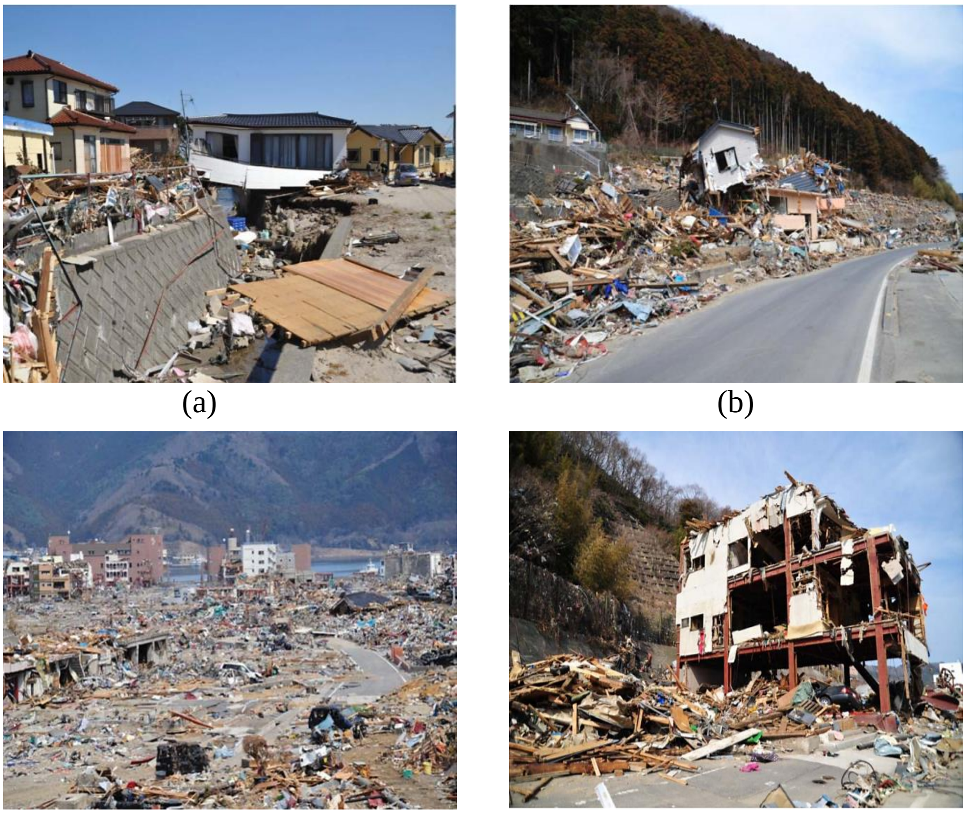

(a) (b) (c) (d)

Figure 2.8 Tsunami impacts on the (a) wood frame residential construction in Iwaki, (b) in Onagawa, (c) engineered reinforced concrete constructions, and (d) steel frame building (Lekkas et al., 2011)

On the other hand, the frames of engineered reinforced concrete structures performed exceptionally well. As shown in Figure 2.8(c), the damage of these building with engineered constructions was minor, and it was limited to broken doors, windows and masonry failures. Similarly, the damage to steel frame buildings was also limited to non-load bearing elements, such as doors, windows or infill walls. In most of the case, the steel frame buildings were left empty of all infill walls, and they were proved to be much vulnerable than the engineered reinforced concrete buildings (Figure 2.8(d)) (Lekkas et al., 2011).

2.2.3 2018 Sulawesi tsunami

In recent year, a massive tsunami, the 2018 Sulawesi tsunami, struck Palu occurred in Indonesia. On 28 September 2018, an earthquake with a magnitude of 7.5 and subsequently a near-field tsunami hit the Bay of Palu and Donggala in the Central of Sulawesi Indonesia 7 minutes to 12 minutes after the earthquake. This major catastrophic tsunami had caused a substantial impact, damage on property, economic loss and loss of life with more than 2000 people died, about 4438 victims with major injuries and 680 people missing (ITIC, 2019). Palu City, Donggala and Sigi are the three most affected region by the tsunami.

A post-tsunami investigation was conducted by the United Nation Educational Scientific and Cultural Organization (UNESCO) international tsunami survey team along 125 km of coastline at the Bay of Palu up to epicenter region. The measurement of tsunami runup height was collected at different surveyed locations, as tabulated in Table 2.3. The findings from the survey report revealed that the observed values for the runup height distribution at survey locations vary from 0.2 m to 9.1 m, in which the maximum runup height of 9.1 m was obtained at Benteng village. Besides accessing the physical parameters related to the tsunami nature, the survey team also explored and analyzed the tsunami impacts on the environment around the affected areas. Along the low-lying coastal regions, massive damage was significantly observed for the building structures, boats, cars and even coastal vegetation.

Table 2.3 Measured tsunami runup height at each region during 2018 Sulawesi tsunami (Omira et al., 2019)

Region	**Maximum tsunami runup height (m)**
Benteng village	9.1
Tanjung Karang	0.2
Donggala city	1.7
Wani	4.8
Bulu Kadia	1.9
Bulu Sigalari	0.9

For instance, the major destruction was suffered in Wani, Panda village, Benteng and Loli-Saluran at the eastern coastline of Palu Bay (Figure 2.9). It was noticed that the boats and cars were swept out by the tsunami waves. There were more than 100 casualties reported from the survey group in Panda. Remarkable destruction on construction and vegetation were witnessed from the tsunami debris along the shoreline. The incident waves even washed away most of the sea-facing houses and only the remaining foundation of the destroyed construction was observed, as shown in Figure 2.10 (Omira et al., 2019). Accordingly, most of the building collapses and structural failures could be assigned to construction deficiencies, improper design and non-ductile detailing.